iScience, Volume *24*

Supplemental information

A shape-deformable liquid-metal-filled magnetorheological plastomer sensor with a magnetic field “on-off” switch

Jiaqi Xu, Haoming Pang, Xinglong Gong, Lei Pei, and Shouhu Xuan

Supplemental Figures

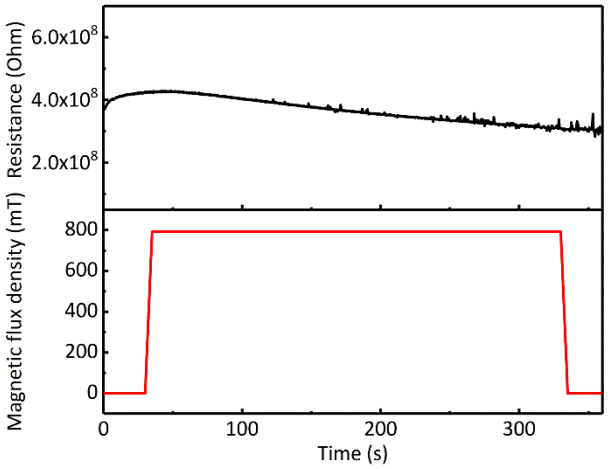

Figure S1. Resistance of LMPU with 24% LM and magnetic flux density over time. Related to Figure 1.

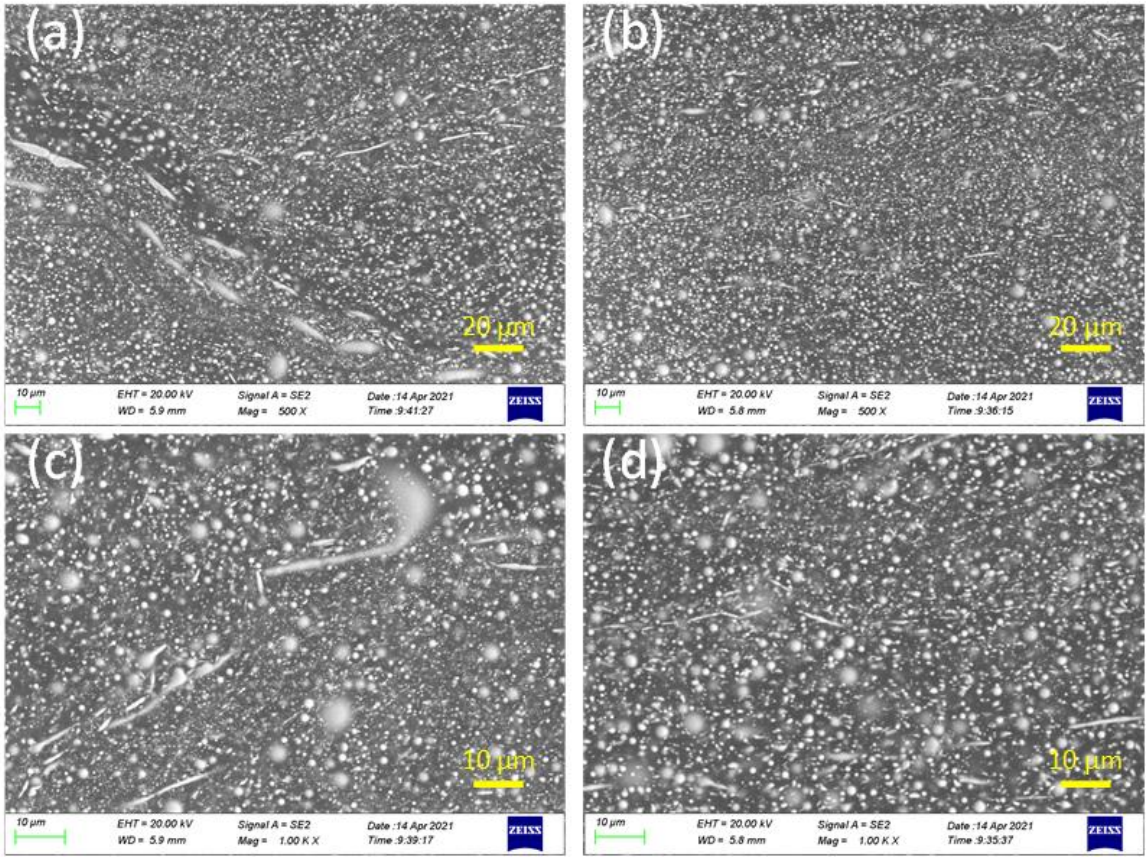

Figure S2. The SEM images of LMPU with 25% LM. Related to Figure 1. The Chamber SE Detector is used and the accelerating voltage is set as 20 kV.

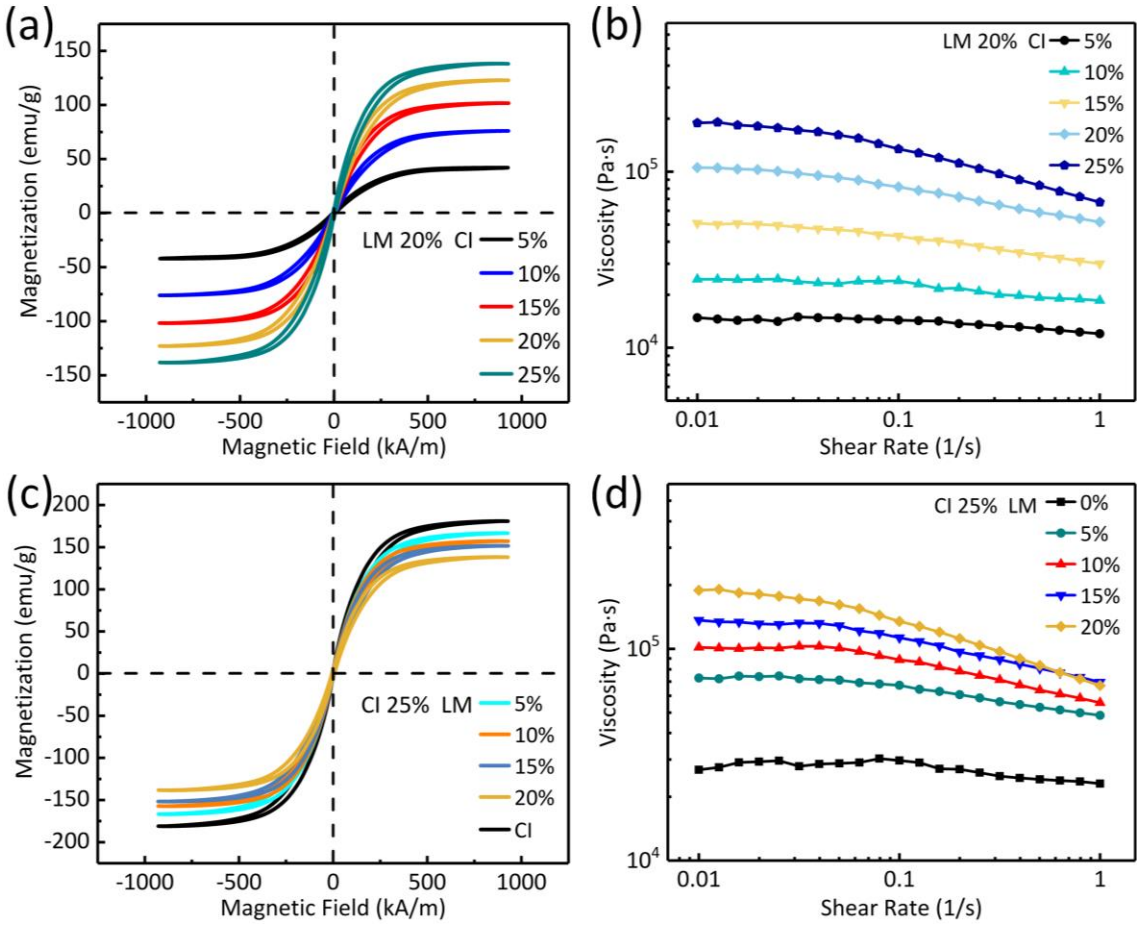

Figure S3. Characterizations of the LMMRPs. Related to Figure 1 (a), (b) Magnetization curves and viscosity of LMMRPs with different CI contents and (c), (d) different LM contents. When the CI volume fraction remains constant at 25%, an increase in LM content means that the mass fraction of CI decreases slightly, so the saturation magnetization of the sample reduces slightly.

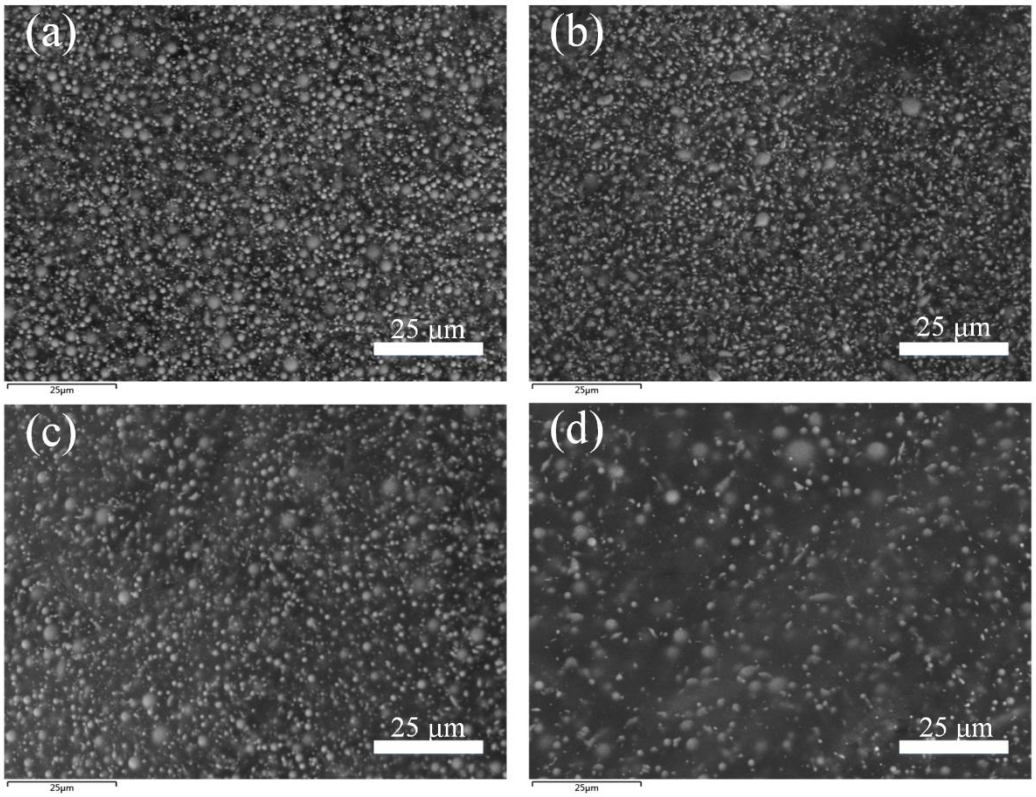

Figure S4. SEM images of LMMRP with 20% LM and different CI contents. Related to Figure 1. (a) 20% CIP, (b) 15% CIP, (c) 10% CIP, and (d) 5% CIP.

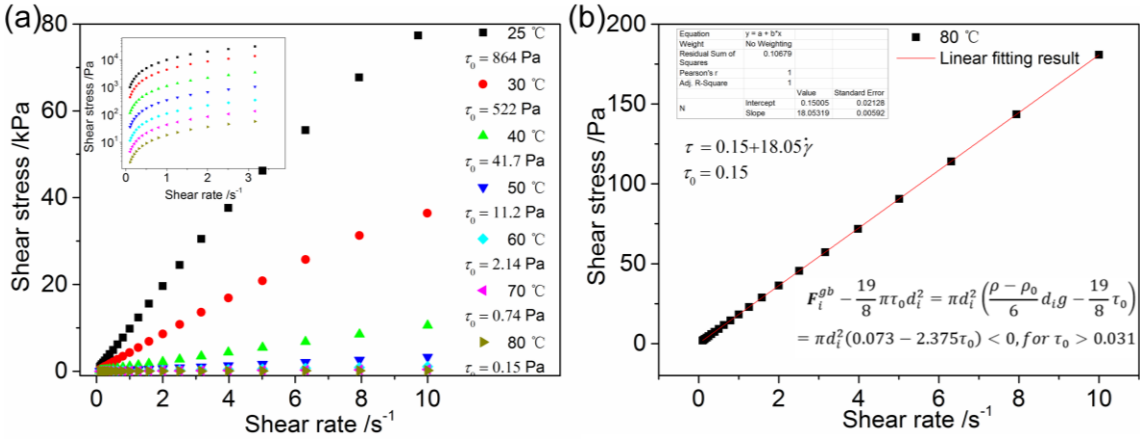

Figure S5. Shear stress-shear rate curves of PU. Related to Figure 7. (a) At different temperatures. (b) Experimental and fitting result of shear stress vs shear rate.

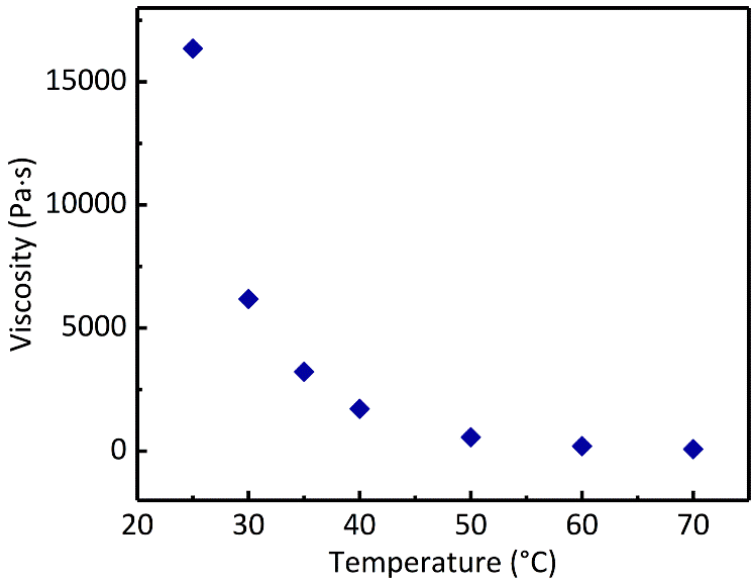

Figure S6. Viscosities of LMPU with 20% LM at different temperatures. Related to Figure 7.

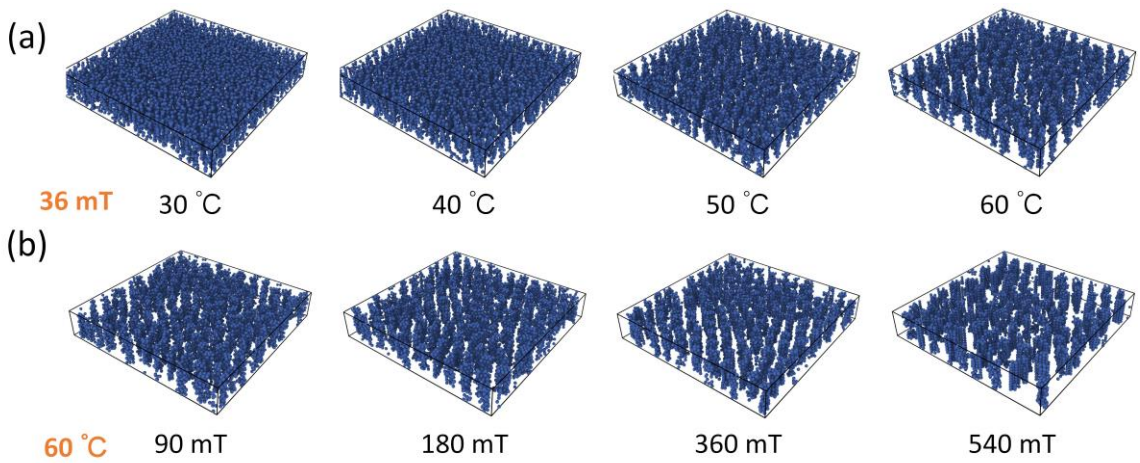

Figure S7. Simulated CI particle structures in LMMRP. Related to Figure 7. (a) At different temperatures. (b) Under different magnetic fields. Here the PU and LM droplets are regarded as a composite matrix.

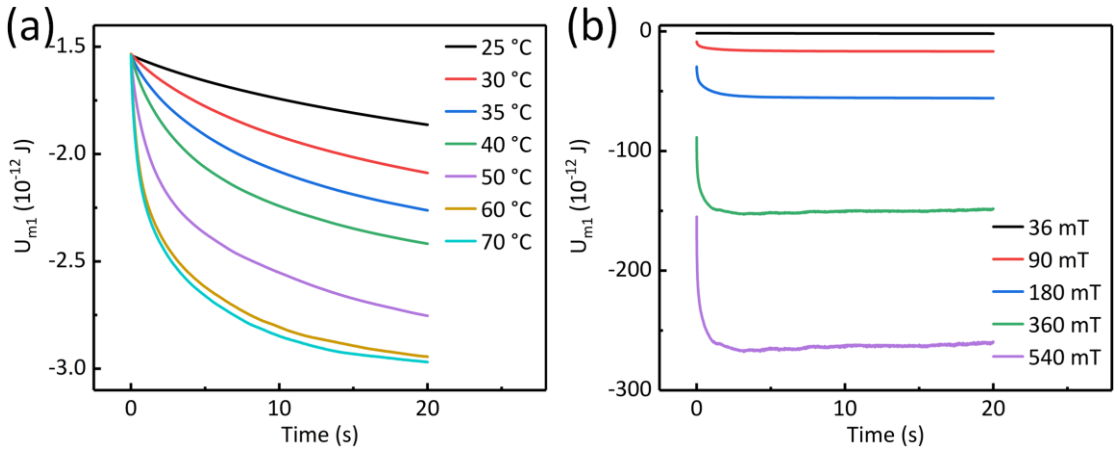

Figure S8. The average magnetic potential energy of each CI particle. Related to Figure 7.
(a) At different temperatures. (b) Under different magnetic fields.